Measurement of Complex Sound Fields – Part 2:

The Use of Lock-In Amplifiers for Phase-Sensitive Measurements of Complex Harmonic Sound Fields

What do Lock-In Amplifiers (*LIA's*) do, and how do they work?

Consider a "generic" experimental situation where a harmonic (*i.e.* periodic/pure-tone/single-frequency) signal of {angular} frequency $\omega = 2\pi f$ is used as a "stimulus" to excite a system (*i.e.* input a known signal into an unknown "black-box"). We are interested in measuring the ***linear***, but possibly ***complex*** response of the "black-box" system to the input stimulus signal – *i.e.* its "output" signal strength (amplitude) and phase of the output signal ***relative*** to the input "stimulus" signal (*aka* the input ***reference*** signal). This "generic" situation is shown in the figure below:

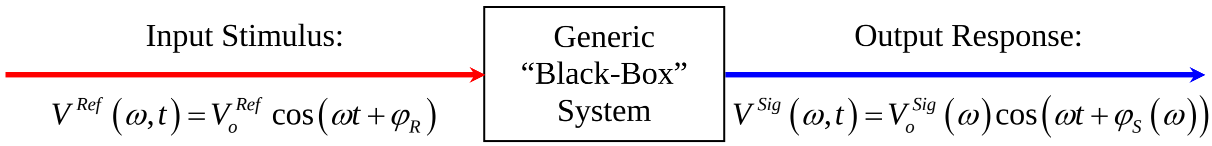

A ***dual-channel*** *LIA* is a narrow-bandwidth electronic device that measures/determines the ***in-phase*** and ***90º-out-of-phase/quadrature amplitude*** components of the response signal output from a generic "black-box" system ***relative*** to a harmonic/pure-tone/single-frequency reference signal input to that system. The generic "black-box" system's output response signal is:

$$V^{Sig}(\omega,t) \equiv V_o^{Sig}(\omega)\cos(\omega t + \varphi_S(\omega)) \text{ of \{angular\} frequency } \omega = 2\pi f\ .$$

Note that in general, both the system's output signal ***amplitude*** $V_o^{Sig}(\omega)$ and ***phase*** $\varphi_S(\omega)$ are frequency-dependent quantities. Whether they in fact are (or are not) depends on the detailed physics associated with how the system's output signal is actually produced, *i.e.* what the output response signal $V^{Sig}(\omega,t)$ physically represents.

Note that the ***in-phase*** and ***90º-out-of-phase/quadrature*** components of the harmonic output response signal ***amplitude*** $V^{Sig}(\omega,t)$ are defined ***relative*** to a ***reference/input*** sine-wave of the same frequency *f*:

$$V^{Ref}(\omega,t) \equiv V_o^{Ref}\cos(\omega t + \varphi_R) \text{ of \{angular\} frequency } \omega = 2\pi f$$

Note further that {here} the ***reference/input*** signal's ***amplitude*** V_o^{Ref} and {absolute} ***phase*** φ_R are both ***constants***, *i.e.* ***time-independent***.

A ***dual-channel*** *LIA* uses ***two*** so-called **Phase-Sensitive Detectors** (*PSD's*) to:

(*a*.) Carry out the mathematical operation of ***multiplication*** of the ***output*** signal with the ***reference/input*** sine-wave signal, and also with a +90° ***phase-shifted copy*** of the ***reference/input*** sine-wave signal, and then:

(*c*.) The two *PSD* ***product*** signals are then either ***time-averaged*** or ***low-pass filtered*** to obtain quasi-*DC* voltages that are representative of the ***in-phase*** and ***90°-out-of-phase/quadrature*** amplitude components of the harmonic (*i.e*. periodic) output response signal, respectively.

The *LIA's* ***reference*** sine-wave signal is:

$$V^{Ref}(\omega,t) = V_o^{Ref}\cos(\omega t + \varphi_R)$$

The +90° ***phase-shifted copy*** of the ***reference*** sine-wave signal is:

$$\begin{aligned} V_{\pi/2}^{Ref}(\omega,t) &= V_o^{Ref}\cos(\omega t + \varphi_R + \pi/2) \\ &= V_o^{Ref}\left[\cos(\omega t + \varphi_R)\cancel{\cos(\pi/2)} - \sin(\omega t + \varphi_R)\sin(\pi/2)\right] \\ &= -V_o^{Ref}\sin(\omega t + \varphi_R) \end{aligned}$$

The generic "black-box" system's output response signal (input to the dual-channel *LIA*) is:

$$V^{Sig}(\omega,t) = V_o^{Sig}(\omega)\cos(\omega t + \varphi_S(\omega))$$

The signal ***multiplication*** operation carried out by the 1st Phase-Sensitive Detector (= PSD_X) is:

$$V^{PSD_X}(\omega,t) \equiv V^{Sig}(\omega,t) \otimes V^{Ref}(\omega,t) = V_o^{Sig}(\omega)\cos(\omega t + \varphi_S(\omega)) \otimes V_o^{Ref}\cos(\omega t + \varphi_R)$$

The signal ***multiplication*** operation carried out by the 2nd Phase-Sensitive Detector (= PSD_Y) is:

$$V^{PSD_Y}(\omega,t) \equiv V^{Sig}(\omega,t) \otimes V_{\pi/2}^{Ref}(\omega,t) = -V_o^{Sig}(\omega)\cos(\omega t + \varphi_S(\omega)) \otimes V_o^{Ref}\sin(\omega t + \varphi_R)$$

We define: $x \equiv \omega t + \varphi_S(\omega)$ and: $y \equiv \omega t + \varphi_R$. Then using Euler's formulas: $\cos x = \tfrac{1}{2}(e^{ix} + e^{-ix})$ and: $\sin x = \tfrac{1}{2i}(e^{ix} - e^{-ix})$, the two *PSD* product terms can be rewritten as:

$$\begin{aligned} \cos x \cos y &= \tfrac{1}{4}(e^{ix} + e^{-ix})(e^{iy} + e^{-iy}) = \tfrac{1}{4}\left(e^{i(x+y)} + e^{-i(x+y)} + e^{i(x-y)} + e^{-i(x-y)}\right) \\ &= \tfrac{1}{4}\left(2\cos(x+y) + 2\cos(x-y)\right) = \tfrac{1}{2}\left(\cos(x+y) + \cos(x-y)\right) \end{aligned}$$

$$\begin{aligned} \cos x \sin y &= \tfrac{1}{4i}(e^{ix} + e^{-ix})(e^{iy} - e^{-iy}) = \tfrac{1}{4i}\left(e^{i(x+y)} - e^{-i(x+y)} - e^{i(x-y)} + e^{-i(x-y)}\right) \\ &= \tfrac{1}{4}\left(2\sin(x+y) - 2\sin(x-y)\right) = \tfrac{1}{2}\left(\sin(x+y) - \sin(x-y)\right) \end{aligned}$$

Thus:

$$V^{PSD_X}(\omega,t) \equiv V^{Sig}(\omega,t) \otimes V^{Ref}(\omega,t)$$
$$= \tfrac{1}{2} V_o^{Sig}(\omega) \cdot V_o^{Ref} \left[\cos\left\{2\omega t + \left(\varphi_S(\omega) + \varphi_R\right)\right\} + \cos\left\{\left(\varphi_S(\omega) - \varphi_R\right)\right\} \right]$$

and:

$$V^{PSD_Y}(\omega,t) \equiv V^{Sig}(\omega,t) \otimes V_{\pi/2}^{Ref}(\omega,t)$$
$$= -\tfrac{1}{2} V_o^{Sig}(\omega) V_o^{Ref} \left[\sin\left\{2\omega t + \left(\varphi_S(\omega) + \varphi_R\right)\right\} - \sin\left\{\left(\varphi_S(\omega) - \varphi_R\right)\right\} \right]$$

Next, we (deliberately) choose to set the ***reference*** amplitude to: $V_o^{Ref} \equiv \sqrt{2} = 1.4142 \ Volts$
{*i.e.* set the ***RMS*** ***reference*** amplitude to: $V_{o_{RMS}}^{Ref} \equiv \tfrac{1}{\sqrt{2}} V_o^{Ref} = 1.0000 \ Volts$ }.

Then, the two *PSD* ***product*** signals become:

$$V^{PSD_X}(\omega,t) \equiv V^{Sig}(\omega,t) \otimes V^{Ref}(\omega,t)$$
$$= +\tfrac{1}{\sqrt{2}} V_o^{Sig}(\omega) \left[\cos\left\{2\omega t + \left(\varphi_S(\omega) + \varphi_R\right)\right\} + \cos\left\{\left(\varphi_S(\omega) - \varphi_R\right)\right\} \right]$$

and:

$$V^{PSD_Y}(\omega,t) \equiv V^{Sig}(\omega,t) \otimes V_{\pi/2}^{Ref}(\omega,t)$$
$$= -\tfrac{1}{\sqrt{2}} V_o^{Sig}(\omega) \left[\sin\left\{2\omega t + \left(\varphi_S(\omega) + \varphi_R\right)\right\} - \sin\left\{\left(\varphi_S(\omega) - \varphi_R\right)\right\} \right]$$

Thus, note that the ***RMS*** output signal amplitude is: $V_{o_{RMS}}^{Sig}(\omega) \equiv \tfrac{1}{\sqrt{2}} V_o^{Sig}(\omega)$

Thus, the two *PSD* ***product*** signals can be expressed in terms of their ***RMS*** amplitudes as:

$$V^{PSD_X}(\omega,t) \equiv V^{Sig}(\omega,t) \otimes V^{Ref}(\omega,t)$$
$$= V_{o_{RMS}}^{Sig}(\omega) \left[\cos\left\{2\omega t + \left(\varphi_S(\omega) + \varphi_R\right)\right\} + \cos\left\{\left(\varphi_S(\omega) - \varphi_R\right)\right\} \right]$$

and:

$$V^{PSD_Y}(\omega,t) \equiv V^{Sig}(\omega,t) \otimes V_{\pi/2}^{Ref}(\omega,t)$$
$$= -V_{o_{RMS}}^{Sig}(\omega) \left[\sin\left\{2\omega t + \left(\varphi_S(\omega) + \varphi_R\right)\right\} - \sin\left\{\left(\varphi_S(\omega) - \varphi_R\right)\right\} \right]$$

Next, we can either ***time-average*** the two *PSD* ***product*** signals, or *e.g.* send them through a {very} ***low-pass filter*** (with –3 *dB* corner frequency $\omega_{-3\,dB} \ll 2\omega$). By doing either of these, we eliminate (*i.e.* ***reject***) the time-dependent/oscillatory (2ω) frequency components of the two *PSD* ***product*** signals; hence only the ***time-independent*** (*i.e.* the zero-frequency) components of the two *PSD* ***product*** signals remain:

$$\left\langle V^{PSD_X}(\omega,t)\right\rangle_t = V_{LPF}^{PSD_X}(\omega) = V_{o_{RMS}}^{S}(\omega)\cos\left(\varphi_S(\omega)-\varphi_R\right)$$

and:

$$\left\langle V^{PSD_Y}(\omega,t)\right\rangle_t = V_{LPF}^{PSD_Y}(\omega) = V_{o_{RMS}}^{S}(\omega)\sin\left(\varphi_S(\omega)-\varphi_R\right)$$

If we now set the {absolute} ***reference*** signal's phase $\varphi_R \equiv 0$, since it ***is*** the ***reference*** phase {*n.b.* we can also eliminate φ_R simply by re-defining the zero of time}, then the two ***time-averaged/LPF 'd time-independent*** *PSD* ***product*** signals simplify further to:

$$\left\langle V^{PSD_X}(\omega,t)\right\rangle_t = V_{LPF}^{PSD_X}(\omega) = V_{o_{RMS}}^{S}(\omega)\cos\varphi_S(\omega)$$

and:

$$\left\langle V^{PSD_Y}(\omega,t)\right\rangle_t = V_{LPF}^{PSD_Y}(\omega) = V_{o_{RMS}}^{S}(\omega)\sin\varphi_S(\omega)$$

Thus, we see that a dual-channel *LIA* enables us to measure the *RMS* values of the ***real/in-phase*** and ***imaginary/90º-out-of-phase/quadrature*** components of a ***periodic*** complex signal ***amplitude***, relative to a ***reference*** sine-wave signal – *i.e.* obtain the ***frequency-domain*** representation of the *RMS* complex harmonic amplitude of a generic "black-box" output response signal, phase-referenced to the input ***reference*** signal:

$$\tilde{V}_{RMS}^{Sig}(\omega) = V_{o_{RMS}}^{Sig}(\omega)\left[\cos\varphi_S(\omega)+i\sin\varphi_S(\omega)\right] = V_{o_{RMS}}^{Sig}(\omega)\cdot e^{i\varphi_S(\omega)}$$

The ***time-domain*** representation of the *RMS* complex harmonic amplitude associated with the generic "black-box" output response signalm phase-referenced to the input ***reference*** signal is:

$$\tilde{V}_{RMS}^{Sig}(\omega,t) = \tilde{V}_{RMS}^{Sig}(\omega)\cdot e^{i\omega t} = \left[\tilde{V}_{o_{RMS}}^{Sig}(\omega)\cdot e^{i\varphi_S(\omega)}\right]\cdot e^{i\omega t} = V_{o_{RMS}}^{Sig}(\omega)\cdot e^{i\left(\omega t+\varphi_S(\omega)\right)}$$

The dual-channel *LIA* is an extremely useful, versatile, sensitive and powerful device. It is routinely used in all sorts of applications involving the measurement and analysis of periodic/pure-tone/single-frequency complex signals.

An important aspect of a *LIA* is that it is inherently a narrow-band frequency device. One sets the bandwidth sensitivity of the *LIA* by specifying its ***settling time constant*** τ (*sec*), which, from the uncertainty relation $\Delta f\,\Delta t = \Delta f\cdot\tau = 1$, sets the *LIA*'s bandwidth: $BW = \Delta f = 1/\tau$. When the ***reference*** signal's frequency changes abruptly $f \to f'$, the system's output ***response*** signal (input to the *LIA*) ***also*** changes abruptly. It is therefore good experimental practice to wait at least Δt ~ 5 time constants in order to allow the *X*, *Y* (***real/in-phase*** and ***imaginary/90-degree-out-of-phase***) outputs of the *LIA* to settle to within $1-e^{-\Delta t/\tau} = 1-e^{-5} \simeq 1-0.007 = 0.993$ of their final values at the new reference frequency f' before recording/reading out the new *X*, *Y* values.

The use of a dual-channel *LIA* for phase-sensitive measurements of periodic complex pressure $\tilde{p}(\vec{r},t)$ and/or particle velocity $\vec{\tilde{u}}(\vec{r},t)$ signals associated with a complex sound field $\tilde{S}(\vec{r},t;\omega)$ has associated with it one other detail which is not immediately apparent in the above formulae.

Consider the use of a dual-channel *LIA* in a typical ***phase-sensitive*** acoustical physics experiment, such as the typical one shown in the figure below, in which a sound source is excited by a pure-tone/single-frequency sine-wave signal output from a function generator, whose instantaneous output voltage is of the form $V^{FG}(\omega,t)=V_o^{FG}\cos(\omega t)$. The sine-wave signal is also used as the ***reference*** for the dual-channel *LIA*.

For simplicity's sake, let us imagine that we have an ***ideal*** sound source, in that it does *not* introduce a phase shift of any kind in the process of generating a monochromatic traveling plane wave, which propagates as a ***free-field***. The ***time-domain*** representation of the complex over-pressure amplitude associated with the ***free-field*** monochromatic traveling plane wave propagating in the *+ve* $\hat{x}$-direction is of the form $\tilde{p}(x,t;\omega)=p_o e^{i(\omega t-kx)}=p_o e^{-ikx}\cdot e^{i\omega t}=\tilde{p}(x,\omega)\cdot e^{i\omega t}$, where $\tilde{p}(x,\omega)$ is the ***frequency-domain*** representation of the complex over-pressure amplitude associated with the monochromatic traveling plane wave.

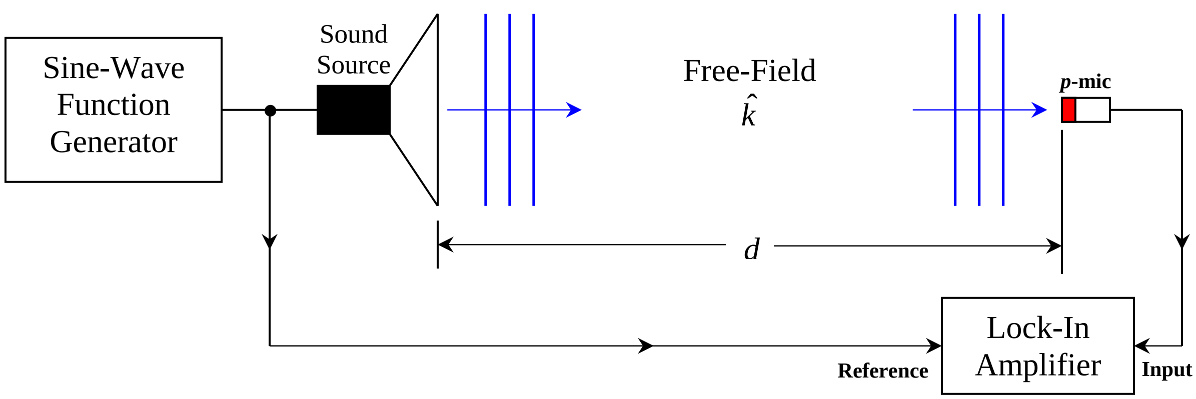

If the pressure mic is located at *x* = 0, then: $\tilde{p}(x=0,t)=p_o\cdot e^{i\omega t}$. The ***real/in-phase*** and ***imaginary/90º-out-of-phase/quadrature*** *RMS* voltage amplitude components output from the *LIA* will be $V_{o_{RMS}}^{Sig}$ and 0, respectively – *i.e.* the phase $\varphi_S|_{x=0}=0$.

If the *p*-mic sensitivity is $S_{p\text{-}mic}(mV/Pascal)$, then the ***frequency-domain real/in-phase*** and ***imaginary/90º-out-of-phase/quadrature*** *RMS* components of the complex pressure amplitude $\tilde{p}(x=0,\omega)$ at *x* = 0 are: $p_o=V_{o_{RMS}}^{Sig}/S_{p\text{-}mic}\ (RMS\ Pascals)$ and: $0\ (RMS\ Pascals)$, respectively.

If the pressure mic is instead moved to *x* = *d*, the complex over-pressure amplitude associated with the ***free-field*** monochromatic traveling plane wave at $x=d$ is:

$$\tilde{p}(x=d,t;\omega)=p_o e^{i(\omega t-kd)}=p_o e^{-ikd}\cdot e^{i\omega t}=p_o[\cos kd-i\sin kd]\cdot e^{i\omega t}=\tilde{p}(x=d,\omega)\cdot e^{i\omega t}$$

Thus, the ***frequency-domain real/in-phase*** and ***imaginary/90º-out-of-phase/quadrature*** *RMS* voltage amplitude components output from the *LIA* for the pressure mic located at *x* = *d* will be:

$V_{o_{RMS}}^{Sig}\cos\varphi_S$ and: $V_{o_{RMS}}^{Sig}\sin\varphi_S$, respectively.

Thus, the ***frequency-domain real/in-phase*** and ***imaginary/90º-out-of-phase/quadrature*** *RMS* components of the complex pressure amplitude $\tilde{p}(x=d,\omega)$ at *x* = *d* are:

$p_o\cos\varphi_S = V_{o_{RMS}}^{Sig}\cos\varphi_S / S_{p\text{-}mic}\;(RMS\ Pascals)$ and:
$p_o\sin\varphi_S = V_{o_{RMS}}^{Sig}\sin\varphi_S / S_{p\text{-}mic}\;(RMS\ Pascals)$, respectively, since: $p_o = V_{o_{RMS}}^{Sig} / S_{p\text{-}mic}$.

Thus, we see that at *x* = *d*, a propagation delay time-induced phase shift of $\varphi_S|_{x=d} = -kd$ results from the fact that it takes a ***finite time*** $\Delta t_{prop} = d/c$ for the a ***free-field*** plane wave to propagate in free air from *x* = 0 to *x* = *d*. Since $k = \omega/c = 2\pi/\lambda$ in free-air, we see that the apparent phase shift at $x = d$ is: $\varphi_S|_{x=d} = -kd = -(\omega/c)\cdot d = -(\omega/c)\cdot(c\Delta t_{prop}) = -\omega\Delta t_{prop}$.

Thus {here}, we see that the phase shift $\varphi_S|_{x=d}$ at $x = d$ is in fact frequency dependent, linearly proportional to the (angular) frequency: $\varphi_S(\omega)|_{x=d} = -k(\omega)d = -\omega\cdot\Delta t_{prop}(\omega)$, becoming more negative with increasing (angular) frequency $\omega = 2\pi f$. See figure below.

While the propagation delay time-induced phase shift effect may initially be perceived as an experimental annoyance, it is actually a physics blessing in disguise!

If the *p*-mic distance *d* from the sound source is known, then a measurement of the ***phase speed*** of sound (the speed at which the phase {*i.e*. the crests/troughs of sound waves} advances) $c_\phi(\omega) \equiv \omega/k(\omega) = f\cdot\lambda(\omega)$ *vs*. frequency *f* can be obtained using:

$$\boxed{c_\phi(\omega) \equiv \omega/k(\omega) = -\left(\omega/\varphi_S(\omega)|_{x=d}\right)\cdot d = -\left(2\pi f/\varphi_S(f)|_{x=d}\right)\cdot d\ \ (m/s)}$$

The ***group speed*** of propagation of sound waves ((the speed at which ***energy/information*** propagates) is defined as: $c_g(\omega) \equiv \left[dk(\omega)/d\omega\right]^{-1}$, which is the {inverse of the} ***local slope*** of the graph of $k(\omega)$ *vs*. ω (at fixed *p*-mic position, *d*). Thus, since $\varphi_S(\omega)|_{x=d} = -k(\omega)d$, then: $d\varphi_S(\omega)|_{x=d}/d\omega = -\left(dk(\omega)/d\omega\right)\cdot d$, hence the ***group speed*** of propagation of sound waves

$$\boxed{c_g(\omega) \equiv \left[dk(\omega)/d\omega\right]^{-1} = d\left[-d\varphi_S(\omega)|_{x=d}/d\omega\right]^{-1}\ (m/s)}$$

For propagation of ***free-field*** monochromatic traveling plane waves, the local slope $dk(\omega)/d\omega = k(\omega)/\omega$, hence $c_g(\omega) = c_\phi(\omega) = \omega/k(\omega)$ in the ***free-field***. In general, this is not the case for an arbitrary sound field, *e.g*. the near *vs*. far zone associated with a point/monopole sound source, or *e.g*. a plane circular piston of radius *a* (an approximation to a loudspeaker).

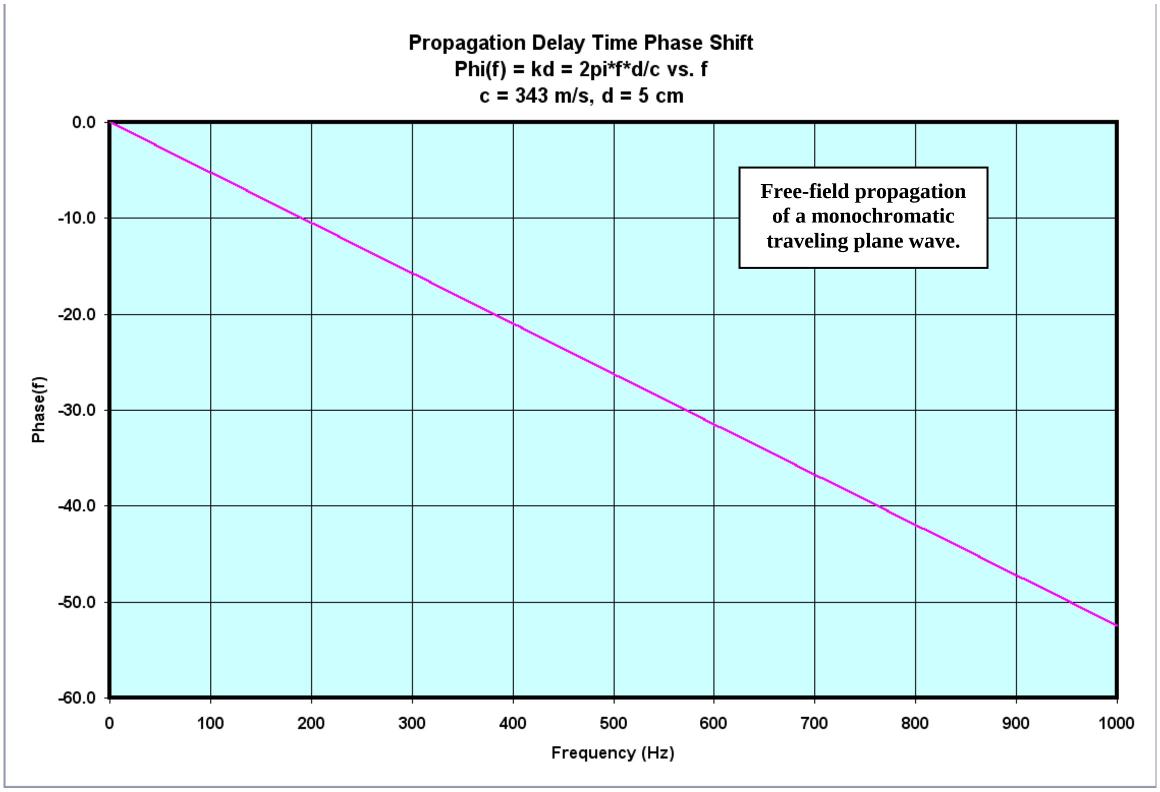

In the UIUC Physics 406 POM lab, we use Stanford Research System's SR-830 Dual-Channel *DSP* Lock-In Amplifiers (one is shown in figure below) to carry out ***phase*-*sensitive*** measurements of the complex pressure $\tilde{p}(\vec{r},t)$ and particle velocity $\vec{\tilde{u}}(\vec{r},t)$ associated with a harmonic/periodic/pure-tone/single-frequency complex sound field $\tilde{S}(\vec{r},t;\omega)$.

SR830 DSP Lock-In Amplifier

A functional block diagram of how the SR-830 *DSP LIA* works is shown in the figure below:

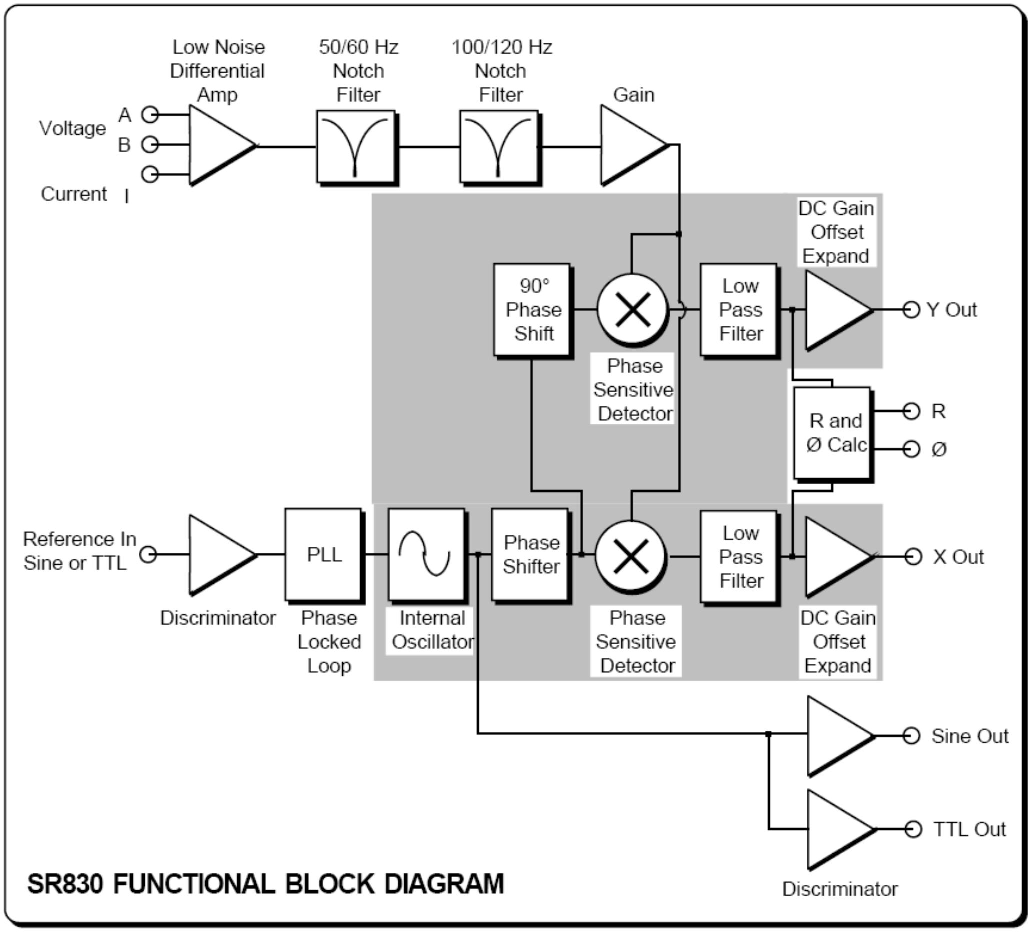

The dual-channel SR-830 DSP LIA is a ***digital*** lock-in amplifier – this means that the voltage waveform of the analog input signal is sampled at a 256 *KHz* digitization rate using a 16-bit analog-to-digital converter. A Phase-Locked Loop (*PLL*) circuit is used to lock the phase of the reference sine-wave (or in the form of a *TTL* digital signal) to an internal 20-bit ***digital*** oscillator. {Or, the internal 20-bit digital oscillator of the SR-830 DSP LIA can be used as the reference sine-wave, programming its amplitude and frequency settings via the GPIB (General Purpose Instrumentation Bus) interface to a PC. The LIA's Digital Signal Processor (*DSP*) then carries out ***all*** of the necessary mathematical operations (multiplication, 90^{o} phase shift, low-pass digital filtering) discussed above, in the ***digital*** domain. This approach is ***vastly*** superior in terms of improved stability, reduced noise, overall performance & flexibility/versatility in comparison to the performance of the ***analog*** lock-in amplifiers of yesteryear… it is truly a powerful device, one which has been used in countless laboratory settings, and in countless physics, engineering, biology, … applications!

Note that the SR-830 *DSP LIA* can also be used to analyze the higher harmonics associated with ***polyphonic*** complex sound fields, consisting of a hierarchy of {***precisely***} integer-related overtones (up to n = 99!).

SR-830 DSP Lock-In Amplifier Specifications

SR810 and SR830 Specifications

Signal Channel

Voltage inputs	Single-ended or differential
Sensitivity	2 nV to 1 V
Current input	10^6 or 10^8 V/A
Input impedance	
Voltage	10 MΩ + 25 pF, AC or DC coupled
Current	1 kΩ to virtual ground
Gain accuracy	±1 % (±0.2 % typ.)
Noise (typ.)	6 nV/√Hz at 1 kHz 0.13 pA/√Hz at 1 kHz (10^6 V/A) 0.013 pA/√Hz at 100 Hz (10^8 V/A)
Line filters	50/60 Hz and 100/120 Hz (Q = 4)
CMRR	100 dB to 10 kHz, decreasing by 6 dB/oct above 10 kHz
Dynamic reserve	>100 dB (without prefilters)
Stability	<5 ppm/°C

Reference Channel

Frequency range	0.001 Hz to 102.4 kHz
Reference input	TTL or sine (400 mVpp min.)
Input impedance	1 MΩ, 25 pF
Phase resolution	0.01° front panel, 0.008° through computer interfaces
Absolute phase error	<1°
Relative phase error	<0.001°
Orthogonality	90° ± 0.001°
Phase noise	
Internal ref.	Synthesized, <0.0001° rms at 1 kHz
External ref.	0.005° rms at 1 kHz (100 ms time constant, 12 dB/oct)
Phase drift	<0.01°/°C below 10 kHz, <0.1°/°C above 10 kHz
Harmonic detection	2F, 3F, ... nF to 102 kHz (n < 19,999)
Acquisition time	(2 cycles + 5 ms) or 40 ms, whichever is larger

Demodulator

Stability	Digital outputs and display: no drift Analog outputs: <5 ppm/°C for all dynamic reserve settings
Harmonic rejection	–90 dB
Time constants	10 µs to 30 ks (6, 12, 18, 24 dB/oct rolloff). Synchronous filters available below 200 Hz.

Internal Oscillator

Range	1 mHz to 102 kHz
Frequency accuracy	25 ppm + 30 µHz
Frequency resolution	4½ digits or 0.1 mHz, whichever is greater
Distortion	–80 dBc (f <10 kHz), –70 dBc (f >10 kHz) @ 1 Vrms amplitude
Amplitude	0.004 to 5 Vrms into 10 kΩ (2 mV resolution), 50 Ω output impedance, 50 mA maximum current into 50 Ω
Amplitude accuracy	1 %
Amplitude stability	50 ppm/°C

Outputs	Sine, TTL (When using an external reference, both outputs are phase locked to the external reference.)

Displays

Channel 1	4½-digit LED display with 40-segment LED bar graph. X, R, X-noise, Aux 1 or Aux 2. The display can also be any of these quantities divided by Aux 1 or Aux 2.
Channel 2 (SR830)	4½-digit LED display with 40-segment LED bar graph. Y, θ, Y-noise, Aux 3 or Aux 4. The display can also be any of these quantities divided by Aux 3 or Aux 4.
Offset	X, Y, R can be offset up to ±105 % of full scale.
Expand	X, Y, R can be expanded by 10× or 100×.
Reference	4½-digit LED display

Inputs and Outputs

CH1 output	X, R, X-noise, Aux 1 or Aux 2, (±10 V), updated at 512 Hz
CH2 output (SR830)	Y, θ, Y-noise, Aux 3 or Aux 4, (±10 V), updated at 512 Hz
X, Y outputs (rear panel)	In-phase and quadrature components (±10 V), updated at 256 kHz.
Aux. A/D inputs	4 BNC inputs, 16-bit, ±10 V, 1 mV resolution, sampled at 512 Hz
Aux. D/A outputs	4 BNC outputs, 16-bit, ±10 V, 1 mV resolution
Sine out	Internal oscillator analog output
TTL out	Internal oscillator TTL output
Data buffer	The SR810 has an 8k point buffer. The SR830 has two 16k point buffers. Data is recorded at rates to 512 Hz and read through the computer interfaces.
Trigger in (TTL)	Trigger synchronizes data recording
Remote preamp	Provides power to the optional SR550, SR552 and SR554 preamps

General

Interfaces	IEEE-488.2 and RS-232 interfaces standard. All instrument functions can be controlled and read through IEEE-488.2 or RS-232 interfaces.
Power	40 W, 100/120/220/240 VAC, 50/60 Hz
Dimensions	17" × 5.25" × 19.5" (WHD)
Weight	23 lbs.
Warranty	One year parts and labor on defects in materials and workmanship

SRS Stanford Research Systems

phone: (408)744-9040
www.thinkSRS.com

Phase-Sensitive Measurements of the Complex Specific Acoustic Input/Output Impedance of Brass/Wind Musical Instruments

The complex longitudinal specific acoustic input and output impedance of brass/wind musical instruments can be measured as a function of frequency via a *PC*-based data-acquisition (*DAQ*) system using a (computer-controlled) sine-wave function generator to excite a piezo-electric disk transducer attached to the mouthpiece *e.g.* of a trumpet, saxophone, clarinet, oboe… in conjunction with the use of pairs of the tiny Knowles Electronics *p*- and *u*-mics that we have developed in the UIUC Physics 406 POM lab to measure complex pressure $\tilde{p}(z,t)$ and longitudinal particle velocity $\tilde{u}_{\parallel}(z,t)$ at the input (*i.e.* mouthpiece) and output (*i.e.* bell-end) of brass/wind musical instruments. The signal output from each mic is input to a SR-830 *DSP LIA*, the real and imaginary components of the complex *RMS* pressure and particle velocity amplitudes, output as quasi-*DC* RMS voltages from the four *LIA*'s used in this experiment are digitized using eight 12-bit analog-to-digital converters (*ADC's*). A block diagram of the *PC*-based *DAQ* setup for these types of measurements is shown in the figure below:

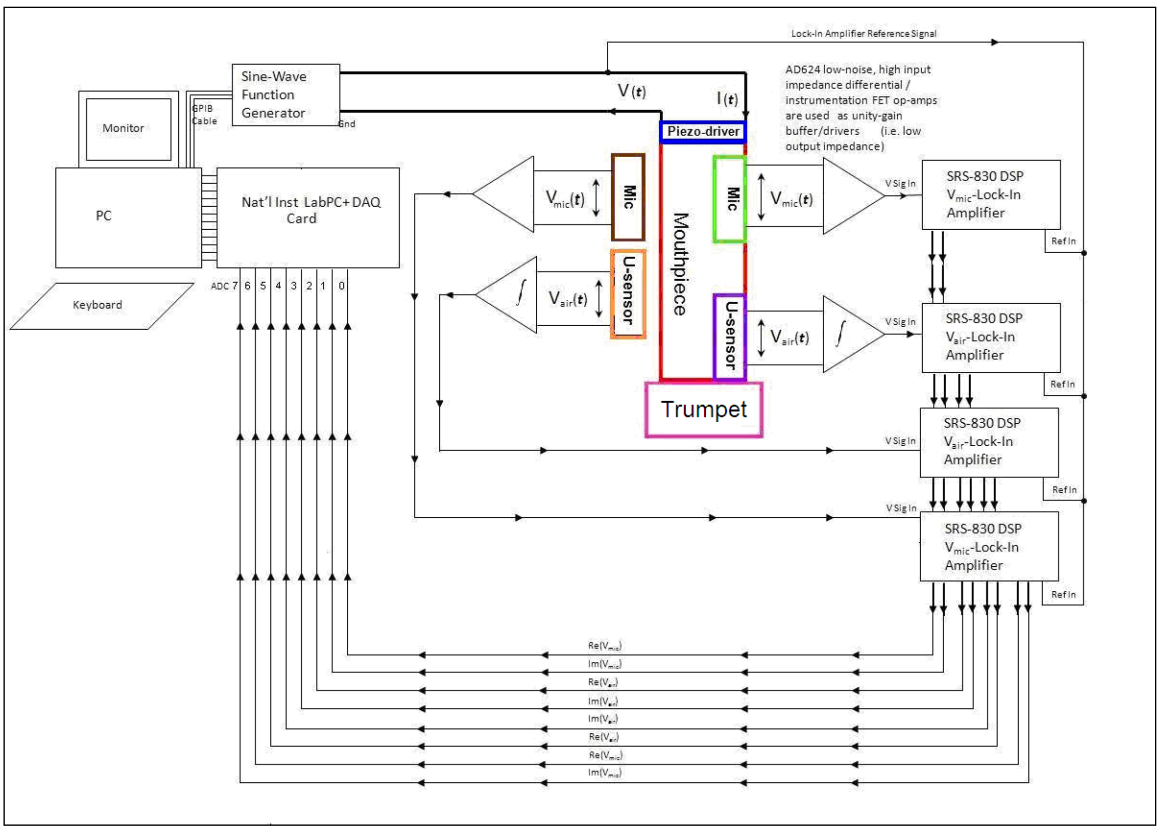

Since we don't have access *e.g.* to an anechoic room, carrying out these measurements in our classroom/lab room is problematic due to 1/*f*-type noise fluctuations from the ventilation system, this unwanted noise can be suppressed by placing the musical instrument to-be-measured in a fairly large, fully-enclosed wooden box lined with acoustic foam on all sides, as shown in the following figure:

A close-up overhead view of the wooden box with a Bach B$_b$ trumpet in it (before the lid is closed):

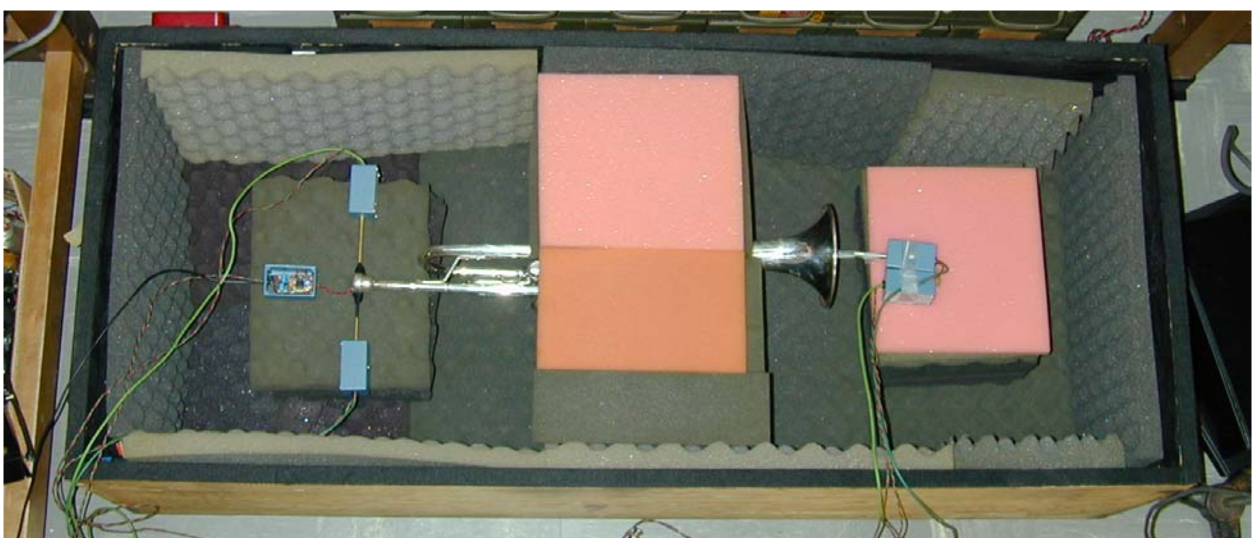

The sensitivities of the *p*- and *u*-mics $S_{p\text{-}mic}$ and $S_{u\text{-}mic}$ are measured/absolutely calibrated in an $SPL = 94\ dB$ free-field sound field, frequency-dependent *p*- and *u*-mic phase corrections are also applied to the raw complex *p*- and *u*-mic data taken for such musical instrument measurements. The complex z_{in} and z_{out} are computed, along with complex I_{in} and I_{out}, resulting in more than 40 individual plots of the real, imaginary, magnitude, phase, cosine of the phase, complex plane associated with complex input/output pressure, complex particle velocity, complex longitudinal specific acoustic impedance and complex longitudinal acoustic intensity.

In the figures below, we show a few of these plots – absolutely calibrated, fully-corrected input (pink) output (blue) $\left|\tilde{p}(f)\right|$, $\left|\tilde{u}_{\parallel}(f)\right|$ and $\left|\tilde{z}_{\parallel}(f)\right|$ data for the Bach B$_b$ trumpet:

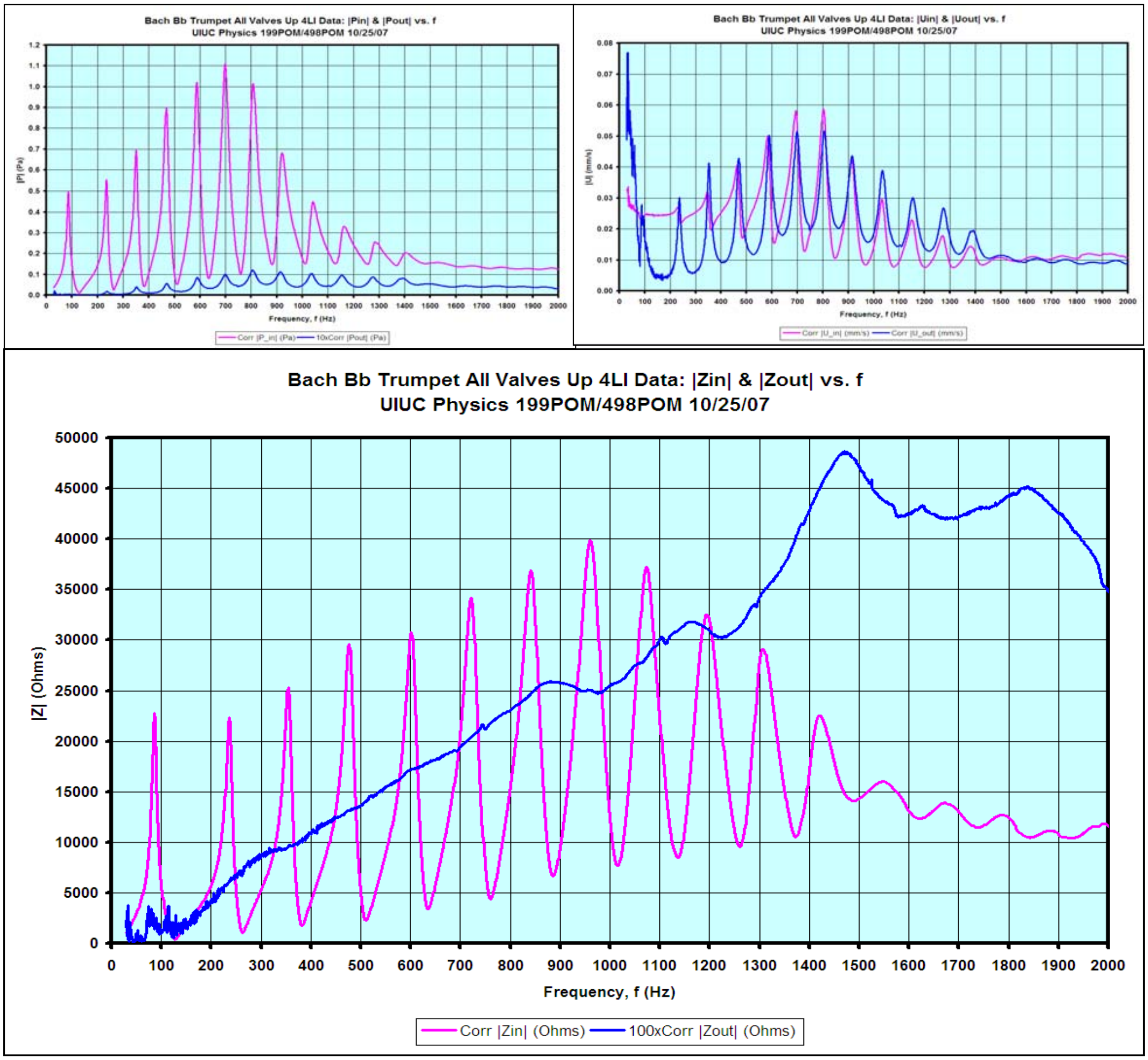

The (pink) input impedance peaks enable a player to play those notes on the trumpet. The lowest ***playable*** note is actually the 2nd peak – the output impedance on the 1st peak is a dead short!

Much more information on the details of these types of measurements and results for various brass/wind musical instruments are posted on the UIUC Physics 406POM website, at:

http://courses.physics.illinois.edu/phys406/406pom_reu.html

The Music Acoustics Group in the Physics Department at The University of New South Wales, in Sydney, Australia has an excellent website http://www.phys.unsw.edu.au/music/ of their very active/on-going musical acoustics physics research program, which also has much interesting information on brass/wind instruments, amongst many other musical instruments.

Spectral Analysis Approach to Measurements of Complex Sound Fields

A complex ***polyphonic*** sound field may consist of ***many*** individual sound fields, each one with its own characteristic frequency {and/or frequencies}, which may {or may not} necessarily be related in phase to other polyphonic components of the overall sound field. The individual components of the overall complex polyphonic sound field may also emanate from their own sound source(s) at different spatial locations. In such situations, measurements of the so-called ***frequency domain power spectral densities*** $\tilde{S}(\vec{r},t;\omega)$ associated with complex overpressure $\tilde{p}(\vec{r},t)$ and particle velocity $\tilde{\vec{u}}(\vec{r},t)$ are carried out in order to determine the nature of the overall sound field at the listener's position $\vec{r}$.

We use Fourier transforms to obtain the ***frequency domain*** complex overpressure $\tilde{p}(\vec{r},\omega)$ and particle velocity $\tilde{\vec{u}}(\vec{r},\omega)$ associated with their ***time domain*** complex overpressure $\tilde{p}(\vec{r},t)$ and particle velocity $\tilde{\vec{u}}(\vec{r},t)$ counterparts.

For any ***continuous***, mathematically ***well-behaved*** complex ***time domain*** function $\tilde{g}(t)$, the Fourier transform of ***time domain*** $\tilde{g}(t)$ to the ***frequency domain*** f (and/or ***angular frequency domain*** $\omega = 2\pi f$) is:

$$\boxed{\tilde{g}(f) = \tilde{g}(\omega) = \mathcal{F}\{\tilde{g}(t)\} \equiv \int_{-\infty}^{+\infty} \tilde{g}(t) e^{-i\omega t} dt = \int_{-\infty}^{+\infty} \tilde{g}(t) e^{-i2\pi f t} dt}$$

The ***inverse*** Fourier transform(s) of ***frequency domain*** $\tilde{g}(f) = \tilde{g}(\omega)$ to the ***time domain*** is:

$$\boxed{\tilde{g}(t) = \mathcal{F}^{-1}\{\tilde{g}(\omega)\} \equiv \tfrac{1}{2\pi}\int_{-\infty}^{+\infty} \tilde{g}(\omega) e^{+i\omega t} d\omega = \int_{-\infty}^{+\infty} \tilde{g}(f) e^{+i2\pi f t} df} \quad \text{since: } \boxed{d\omega = 2\pi \cdot df}$$

Note that the choice of the $\pm$ signs in the complex exponential factors in the above Fourier transform expressions is ***not*** arbitrary – long ago, we specified the $e^{+i\omega t}$ convention for use in our physically-measureable quantities, *e.g.* $\tilde{p}(t) = p_o e^{+i\omega t}\ (Pascals)$, $\tilde{u}_{\|}(t) = u_{\|}^{o} e^{+i\omega t}\ \left(m/sec^{-1}\right)$, *etc.*

A Simple Example of the Use of Fourier Transforms:

Suppose we have a pure-tone/single frequency $(\omega \equiv \omega_o = 2\pi f_o)$ complex ***time domain*** signal $\tilde{g}(t) = p_o e^{+i\omega_o t}\ (Pascals)$, where, for simplicity's sake {***here***}, the overpressure amplitude $p_o\ (Pascals)$ is a purely real number (*i.e.* a constant). Depending on the physical quantity that the ***time domain*** signal $\tilde{g}(t)$ actually represents, the ***time domain*** signal $\tilde{g}(t)$ has dimensionful physical units associated with it – *e.g. RMS Volts*, *Pascals*, *meters/second*, *etc.*

Hence, note that the physical units associated with the ***frequency domain*** Fourier transform of $\tilde{g}(t)$, $\tilde{g}(f) = \mathcal{F}\{\tilde{g}(t)\} \equiv \int_{-\infty}^{+\infty} \tilde{g}(t) e^{-i2\pi f t} dt$ will correspondingly be *RMS Volt-sec*, *Pascal-*

sec, *meters*, *etc*. However, since frequencies (f) are usually expressed in *Hz* (= cycles per second = *sec*$^{-1}$), the dimensionful physical units of ***frequency domain*** $\tilde{g}(f)$ are more commonly expressed as *RMS Volts/Hz, Pascals/Hz,* (*meters/sec*)*/Hz, etc*., respectively.

The ***angular frequency*** Fourier transform of $\tilde{g}(t)$, $\tilde{g}(\omega) = \mathcal{F}\{\tilde{g}(t)\} \equiv \int_{-\infty}^{+\infty} \tilde{g}(t) e^{-i\omega t} dt$ have dimensionful physical units of *RMS Volt*-sec/*rad, Pascal-sec*/*rad, meters*/*rad, etc*., respectively.

If we now explicitly insert $\tilde{g}(t) = p_o e^{+i\omega_o t}$ into the expression for the Fourier transform of the ***time domain*** $\tilde{g}(t)$ to the ***frequency domain***:

$$\tilde{g}(\omega) = \mathcal{F}\{\tilde{g}(t)\} \equiv \int_{-\infty}^{+\infty} \tilde{g}(t) e^{-i\omega t} dt = \int_{-\infty}^{+\infty} p_o e^{+i\omega_o t} e^{-i\omega t} dt = p_o \underbrace{\int_{-\infty}^{+\infty} e^{+i(\omega_o - \omega)t} dt}_{=2\pi\delta(\omega_o - \omega)} = p_o \cdot 2\pi\delta(\omega_o - \omega)$$

where the delta function $\delta(\omega_o - \omega) = \frac{1}{2\pi}\int_{-\infty}^{+\infty} e^{i(\omega_o - \omega)t} dt$, has the dimensionful physical units of the ***inverse*** of its argument, *i.e*. $1/\omega = 1/2\pi f$ (= seconds/radian, or equivalently, 1/*radian-Hz*).

We insert the ***frequency domain*** $\tilde{g}(\omega) = p_o \cdot 2\pi\delta(\omega_o - \omega)$ into the expression for the ***inverse*** Fourier transform to obtain the ***time domain*** representation $\tilde{g}(t)$:

$$\tilde{g}(t) = \mathcal{F}^{-1}\{\tilde{g}(\omega)\} \equiv \frac{1}{2\pi}\int_{-\infty}^{+\infty} \tilde{g}(\omega) e^{+i\omega t} d\omega = \frac{1}{\cancel{2\pi}}\int_{-\infty}^{+\infty} p_o \cdot \cancel{2\pi}\,\delta(\omega_o - \omega) e^{+i\omega t} d\omega = p_o e^{+i\omega_o t}$$

where we have used the relations: $\int_{-\infty}^{+\infty} \delta(x_o - x) dx = 1$ and: $\int_{-\infty}^{+\infty} g(x) \cdot \delta(x_o - x) dx = g(x_o)$.

Thus, we see that an infinitely long/continuous complex exponential ***time domain*** signal $\tilde{g}(t) = p_o e^{+i\omega_o t}$ corresponds to an infinitely sharp/narrow "spike" in the ***frequency domain*** $\tilde{g}(\omega) = p_o \cdot 2\pi\delta(\omega_o - \omega)$, as shown graphically in the two figures below:

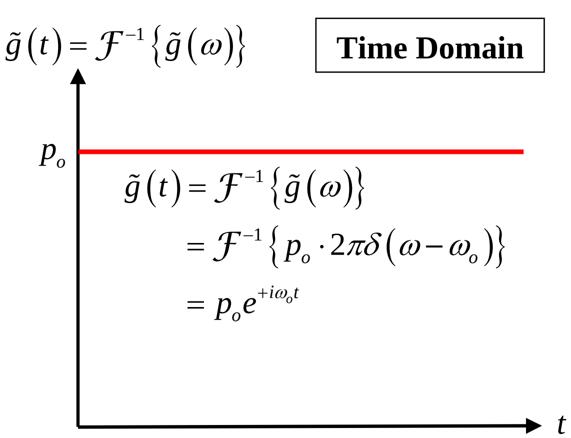

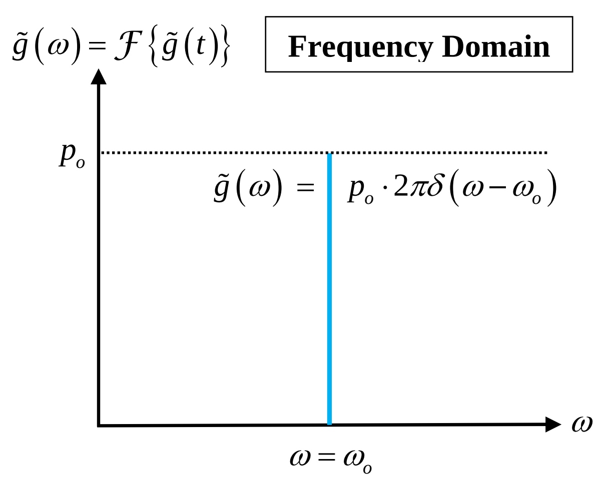

Conversely, an infinitely sharp/narrow ***time*** ***domain*** sound "spike" $\tilde{g}_1(t) = p_o\delta(t)$ $(Pascals/sec)$ produces a ***flat*** frequency ***spectrum*** (a ***continuum*** of frequencies with ***equal*** amplitudes) $\tilde{g}(f) = \tilde{g}(\omega) = \mathcal{F}\{\tilde{g}(t)\} = p_o$ $(Pascals)$, as shown graphically in the two figures below:

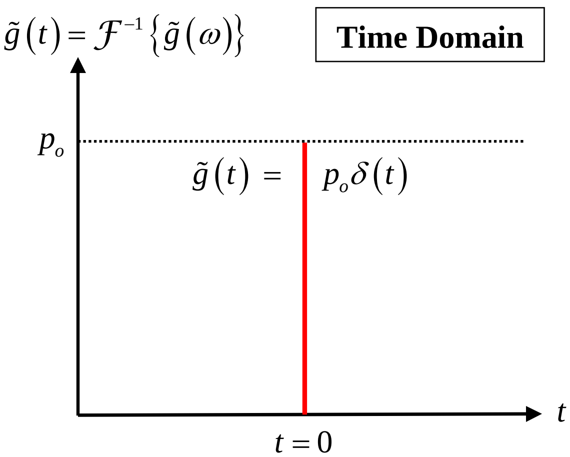

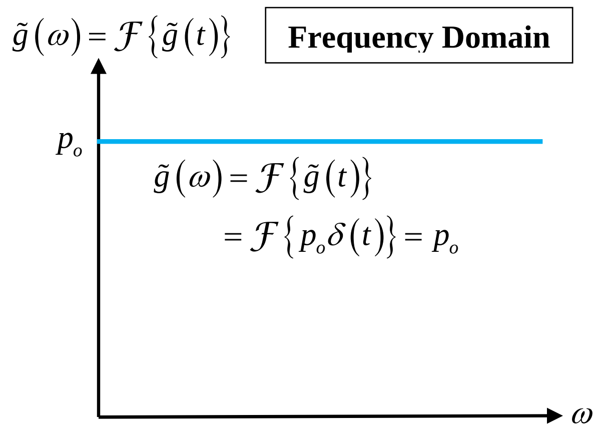

There are many useful relations associated with Fourier transforms, which we summarize below, for the most commonly used ones:

	Time-Domain:		**Frequency Domain:**
Linearity:	$\tilde{h}(t) = a\tilde{f}(t) + b\tilde{g}(t)$	$\Rightarrow$	$\tilde{h}(\omega) = a\tilde{f}(\omega) + b\tilde{g}(\omega)$
Translation:	$\tilde{h}(t) = \tilde{f}(t - t_o)$	$\Rightarrow$	$\tilde{h}(\omega) = \tilde{f}(\omega)e^{i\omega t_o}$
Modulation:	$\tilde{h}(t) = \tilde{f}(t)e^{i\omega_o t}$	$\Rightarrow$	$\tilde{h}(\omega) = \tilde{f}(\omega - \omega_o)$
Scaling:	$\tilde{h}(t) = \tilde{f}(at)$	$\Rightarrow$	$\tilde{h}(\omega) = \frac{1}{\lvert a \rvert}\tilde{f}\left(\frac{\omega}{a}\right)$
Conjugation:	$\tilde{h}(t) = \tilde{f}^*(t)$	$\Rightarrow$	$\tilde{h}(\omega) = \tilde{f}^*(-\omega)$

Discrete Fourier Transforms:

In an experimental/laboratory situation *e.g.* using modern data acquisition hardware such as a digital oscilloscope/digital recorder, or a dedicated waveform acquisition system, where ***time domain*** signals $\tilde{f}(t)$ are ***digitized*** at a constant sampling rate of f_s (samples/second) {corresponding to a sampling time interval $\Delta t_s = 1/f_s$} their ***frequency domain*** counterparts $\tilde{g}(\omega)$ can be obtained using so-called ***discretize***d Fast-Fourier Transform {*FFT*} techniques.

For ***discretized*** complex ***time domain*** functions consisting of a uniformly time-sampled sequence of *N* ***complex*** numbers $\tilde{g}_n(t_n)$, the ***discrete*** Fourier transform of complex ***time domain*** $\tilde{g}_n(t_n)$ to the ***frequency domain*** is: $\tilde{g}_k(\omega_k) = \sum_{n=0}^{N-1} \tilde{g}_n(t_n) e^{-(2\pi i/N)kn}$, with k = 0, 1, 2, …N–1. The ***inverse*** of the ***discrete*** Fourier transform of complex ***frequency domain*** $\tilde{g}_k(\omega_k)$ to the ***time domain*** is: $\tilde{g}_n(t_n) = \frac{1}{N}\sum_{k=0}^{N-1} \tilde{g}_k(\omega_k) e^{+(2\pi i/N)kn}$. The $e^{(2\pi i/N)}$ are known as the ***primitive N^th^ roots of unity***.

For the remainder of the discussion(s) ***here***, we will work with ***continuous*** complex functions $\tilde{g}(t)$ and. We leave it to the interested reader to transcribe the following results to the discretized versions, if needed, or, one can simply consult a good text book on digital signal processing…

Convolution:

We can ***convolute*** a complex ***time domain*** function $\tilde{f}(t)$ with another $\tilde{g}(t)$ by carrying out the mathematical operation of ***convolution***:

$$\boxed{\tilde{h}_{f\otimes g}(t) \equiv \tilde{f}(t) \otimes \tilde{g}(t) \equiv \int_{-\infty}^{+\infty} \tilde{f}(\tau)\cdot \tilde{g}(t-\tau)\, d\tau}$$

The $\otimes$ symbol denotes the ***convolution*** operation. *n.b.* $\tilde{h}(t)$ has units of $\tilde{f}(t)\cdot\tilde{g}(t)\cdot sec$.

The Fourier transform the above relation is: $\tilde{h}_{f\otimes g}(\omega) = \mathcal{F}\left\{\tilde{h}_{f\otimes g}(t)\right\} \equiv \int_{-\infty}^{+\infty} \tilde{h}_{f\otimes g}(t) e^{-i\omega t} dt$, the ***frequency domain*** representation of complex ***time domain convolution***. It can be shown that:

$$\boxed{\tilde{h}_{f\otimes g}(\omega) = \mathcal{F}\left\{\tilde{h}_{f\otimes g}(t)\right\} = \mathcal{F}\left\{\tilde{f}(t)\otimes\tilde{g}(t)\right\} = \mathcal{F}\left\{\tilde{f}(t)\right\}\cdot\mathcal{F}\left\{\tilde{g}(t)\right\} = \tilde{f}(\omega)\cdot\tilde{g}(\omega)}$$

The $\cdot$ symbol denotes simple ***multiplication***. *n.b.* $\tilde{h}_{f\otimes g}(\omega)$ has physical units of $\tilde{f}(\omega)\cdot\tilde{g}(\omega)$.

We see that ***convolution*** of two complex ***time domain*** functions $\tilde{f}(t)\otimes\tilde{g}(t)$ is equivalent to simple ***multiplication*** of their ***frequency domain*** counterparts, $\tilde{f}(\omega)\cdot\tilde{g}(\omega)$!

Cross-Correlation:

The ***cross-correlation*** of a complex ***time domain*** function $\tilde{f}(t)$ with another $\tilde{g}(t)$ is a specialized type of ***convolution***, involving complex conjugation:

$$\boxed{\tilde{h}_{f\star g}(t) \equiv \tilde{f}(t)\star\tilde{g}(t) = \tilde{f}^*(-t)\otimes\tilde{g}(t) = \int_{-\infty}^{+\infty}\tilde{f}^*(-\tau)\cdot\tilde{g}(t-\tau)\,d\tau = \int_{-\infty}^{+\infty}\tilde{f}^*(\tau)\cdot\tilde{g}(t+\tau)\,d\tau}$$

The $\star$ symbol denotes the ***cross-correlation*** operation. *n.b.* $\tilde{h}_{f\star g}(t)$ has units of $\tilde{f}(t)\cdot\tilde{g}(t)\cdot sec$.

The Fourier transform of the ***cross-correlation*** relation is: $\tilde{h}_{f\star g}(\omega) = \mathcal{F}\left\{\tilde{h}_{f\star g}(t)\right\} \equiv \int_{-\infty}^{+\infty}\tilde{h}_{f\star g}(t)e^{-i\omega t}dt$, the ***frequency domain*** representation of complex ***time domain cross-correlation***. It can be shown that:

$$\boxed{\tilde{h}_{f\star g}(\omega) = \mathcal{F}\left\{\tilde{h}_{f\star g}(t)\right\} = \mathcal{F}\left\{\tilde{f}^*(-t)\otimes\tilde{g}(t)\right\} = \mathcal{F}\left\{\tilde{f}^*(-t)\right\}\cdot\mathcal{F}\left\{\tilde{g}(t)\right\} = \tilde{f}^*(\omega)\cdot\tilde{g}(\omega)}.$$

The $\cdot$ symbol denotes simple ***multiplication***. *n.b.* $\tilde{h}_{f\star g}(\omega)$ has physical units of $\tilde{f}^*(\omega)\cdot\tilde{g}(\omega)$.

Auto-Correlation (*aka* Self-Correlation):

Note that the ***auto-correlation*** of a complex time-domain function $\tilde{f}(t)$ with ***itself*** is simply a specialized type of ***cross-correlation***, also involving complex conjugation:

$$\boxed{\tilde{h}_{f\star f}(t) \equiv \tilde{f}(t)\star\tilde{f}(t) = \tilde{f}^*(-t)\otimes\tilde{f}(t) = \int_{-\infty}^{+\infty}\tilde{f}^*(-\tau)\cdot\tilde{f}(t-\tau)\,d\tau = \int_{-\infty}^{+\infty}\tilde{f}^*(\tau)\cdot\tilde{f}(t+\tau)\,d\tau}$$

The Fourier transform of the ***auto-correlation*** relation is: $\tilde{h}_{f\star f}(\omega) = \mathcal{F}\left\{\tilde{h}_{f\star f}(t)\right\} \equiv \int_{-\infty}^{+\infty}\tilde{h}_{f\star f}(t)e^{-i\omega t}dt$, the ***frequency domain*** representation of complex ***time domain auto-correlation***. It can be shown that:

$$\boxed{\tilde{h}_{f\star f}(\omega) = \mathcal{F}\left\{\tilde{h}_{f\star f}(t)\right\} = \mathcal{F}\left\{\tilde{f}(t)\star\tilde{f}(t)\right\} = \mathcal{F}\left\{\tilde{f}^*(-t)\otimes\tilde{f}(t)\right\} = \mathcal{F}\left\{\tilde{f}^*(-t)\right\}\cdot\mathcal{F}\left\{\tilde{f}(t)\right\} = \tilde{f}^*(\omega)\cdot\tilde{f}(\omega)}$$

Note that $\tilde{h}_{f\star f}(t)$ has physical units of $\tilde{f}(t)\cdot\tilde{f}(t)\cdot sec$; $\tilde{h}_{f\star f}(\omega)$ has physical units of $\tilde{f}^*(\omega)\cdot\tilde{f}(\omega)$.

The Weiner-Khintchine Theorem:

The ***Weiner-Khintchine Theorem*** relates the ***time domain auto-correlation*** function $\tilde{h}_{f\star f}(t)$ to the ***frequency domain power spectral density*** function $\tilde{S}_{f\star f}(\omega)$ (and vice versa) via the following Fourier transforms:

$$\boxed{\tilde{S}_{f\star f}(\omega) = \int_{-\infty}^{+\infty}\tilde{h}_{f\star f}(t)e^{-i\omega t}dt} \text{ and: } \boxed{\tilde{h}_{f\star f}(t) = \tfrac{1}{2\pi}\int_{-\infty}^{+\infty}\tilde{S}_{f\star f}(\omega)e^{+i\omega t}d\omega}.$$

These results can be generalized to:

$$\boxed{\tilde{S}_{f\star g}(\omega) = \int_{-\infty}^{+\infty}\tilde{h}_{f\star g}(t)e^{-i\omega t}dt} \text{ and: } \boxed{\tilde{h}_{f\star g}(t) = \tfrac{1}{2\pi}\int_{-\infty}^{+\infty}\tilde{S}_{f\star g}(\omega)e^{+i\omega t}d\omega}.$$

Power Spectral Density Functions:

The ***power spectral density functions*** $\tilde{S}_{p\star p}(\omega)$ and $\tilde{S}_{u\star u}(\omega)$ (*n.b.* complex ***scalar*** quantities) associated with complex scalar pressure $\tilde{p}(\vec{r},t)$ and vector particle velocity $\vec{\tilde{u}}(\vec{r},t)$ are respectively:

$$\boxed{\tilde{S}_{p\star p}(\omega)=\int_{-\infty}^{+\infty}\tilde{h}_{p\star p}(t)e^{-i\omega t}dt=\int_{-\infty}^{+\infty}\left[\int_{-\infty}^{+\infty}\tilde{p}^*(\tau)\cdot\tilde{p}(t+\tau)d\tau\right]e^{-i\omega t}dt=\tilde{p}^*(\omega)\cdot\tilde{p}(\omega)=\left|\tilde{p}(\omega)\right|^2}$$

and: $$\boxed{\tilde{S}_{u\star u}(\omega)=\int_{-\infty}^{+\infty}\tilde{h}_{u\star u}(t)e^{-i\omega t}dt=\int_{-\infty}^{+\infty}\left[\int_{-\infty}^{+\infty}\vec{\tilde{u}}^*(\tau)\bullet\vec{\tilde{u}}(t+\tau)d\tau\right]e^{-i\omega t}dt=\vec{\tilde{u}}^*(\omega)\bullet\vec{\tilde{u}}(\omega)=\left|\vec{\tilde{u}}(\omega)\right|^2}$$

Explicitly writing out the latter relation in terms of its *x*, *y*, and *z*-components:

$$\boxed{\tilde{S}_{u\star u}(\omega)=\left|\vec{\tilde{u}}(\omega)\right|^2}\Rightarrow\boxed{\tilde{S}_{u_x\star u_x}(\omega)+\tilde{S}_{u_y\star u_y}(\omega)+\tilde{S}_{u_z\star u_z}(\omega)=\left|\tilde{u}_x(\omega)\right|^2+\left|\tilde{u}_y(\omega)\right|^2+\left|\tilde{u}_z(\omega)\right|^2}$$

The dimensionful physical units of $\tilde{S}_{p\star p}(f)$ and $\tilde{S}_{u\star u}(f)$ are Pa^2/Hz and $(m/s)^2/Hz$, respectively.
The dimensionful physical units of $\tilde{S}_{p\star p}(\omega)$ and $\tilde{S}_{u\star u}(\omega)$ are Pa^2-s/rad and $(m/s)^2$-s/rad, respectively.
We also see that the 3-D vector ***power spectral density functions*** $\vec{\tilde{S}}_{p\star u}(\omega)$ and $\vec{\tilde{S}}_{u\star p}(\omega)$ – related to the ***frequency-domain*** complex 3-D vector acoustic intensity $\vec{\tilde{I}}_a(\omega)=\frac{1}{2}p(\omega)\cdot\vec{\tilde{u}}^*(\omega)$ are:

$$\boxed{\vec{\tilde{S}}_{p\star u}(\omega)=\int_{-\infty}^{+\infty}\vec{\tilde{h}}_{p\star u}(t)e^{-i\omega t}dt=\int_{-\infty}^{+\infty}\left[\int_{-\infty}^{+\infty}\tilde{p}^*(\tau)\cdot\vec{\tilde{u}}(t+\tau)d\tau\right]e^{-i\omega t}dt=\tilde{p}^*(\omega)\cdot\vec{\tilde{u}}(\omega)}$$

and: $$\boxed{\vec{\tilde{S}}_{u\star p}(\omega)=\int_{-\infty}^{+\infty}\vec{\tilde{h}}_{u\star p}(t)e^{-i\omega t}dt=\int_{-\infty}^{+\infty}\left[\int_{-\infty}^{+\infty}\vec{\tilde{u}}^*(\tau)\cdot\tilde{p}(t+\tau)d\tau\right]e^{-i\omega t}dt=\vec{\tilde{u}}^*(\omega)\cdot\tilde{p}(\omega)}$$

Note that: $\boxed{\left\{\vec{\tilde{S}}_{u\star p}(\omega)=\vec{\tilde{u}}^*(\omega)\cdot\tilde{p}(\omega)\right\}=\left\{\vec{\tilde{S}}_{p\star u}(\omega)=\tilde{p}^*(\omega)\cdot\vec{\tilde{u}}(\omega)\right\}^*=\left\{\vec{\tilde{S}}^*_{p\star u}(\omega)=\tilde{p}(\omega)\cdot\vec{\tilde{u}}^*(\omega)\right\}}$.

Note also that for $x,y=u,p$: $\boxed{\mathrm{Re}\left\{\tilde{S}_{x\star y}(\omega)\right\}=\mathrm{Re}\left\{\tilde{S}_{x\star y}(-\omega)\right\}}$ whereas: $\boxed{\mathrm{Im}\left\{\tilde{S}_{x\star y}(\omega)\right\}=-\mathrm{Im}\left\{\vec{\tilde{S}}_{x\star y}(-\omega)\right\}}$.

The dimensionful physical units of $\tilde{S}_{p\star u}(f)$ and $\tilde{S}_{u\star p}(f)$ are *Watts/m*^{2}*/Hz*.
The dimensionful physical units of $\tilde{S}_{p\star u}(\omega)$ and $\tilde{S}_{u\star p}(\omega)$ are *Watt-s/m*^{2}*/rad*.

Generically, the ***power spectral density functions*** $\tilde{S}_{x\star y}(\omega)$ are defined for ***all*** positive ***and*** negative frequencies, and as such, each $\tilde{S}_{x\star y}(\omega)$ can be represented by ***pairs*** of ***counter-rotating phasors*** in the ***complex plane***.

For practical purposes, it is useful/convenient to redefine the complex ***power*** ***spectral*** ***density*** ***functions*** as ***single-sided*** functions of frequency:

$$\tilde{G}_{x\star y}(\omega) \equiv 2\tilde{S}_{x\star y}(\omega) \text{ for } \omega > 0$$
$$\tilde{G}_{x\star y}(0) \equiv \tilde{S}_{x\star y}(0) \text{ for } \omega = 0$$
$$\tilde{G}_{x\star y}(\omega) \equiv 0 \text{ for } \omega < 0$$

Thus for $\omega > 0$:

$$\tilde{G}_{p\star p}(\omega) \equiv 2\tilde{S}_{p\star p}(\omega) = 2\left|\tilde{p}(\omega)\right|^2 \text{ \{\textit{n.b.} a purely \underline{\textit{real}} quantity!\}}$$

$$\tilde{G}_{u\star u}(\omega) \equiv 2\tilde{S}_{u\star u}(\omega) = 2\left|\vec{\tilde{u}}(\omega)\right|^2 = 2\left[\left|\tilde{u}_x(\omega)\right|^2 + \left|\tilde{u}_y(\omega)\right|^2 + \left|\tilde{u}_z(\omega)\right|^2\right]$$
$$= \tilde{G}_{u_x\star u_x}(\omega) + \tilde{G}_{u_y\star u_y}(\omega) + \tilde{G}_{u_z\star u_z}(\omega) \text{ \{\textit{n.b.} a purely \underline{\textit{real}} quantity!\}}$$

$$\vec{\tilde{G}}_{p\star u}(\omega) \equiv 2\vec{\tilde{S}}_{p\star u}(\omega) = 2\tilde{p}^*(\omega)\cdot\vec{\tilde{u}}(\omega) \text{ \{\textit{n.b.} in general, complex\}}$$
$$= \tilde{G}_{p\star u_x}(\omega)\hat{x} + \tilde{G}_{p\star u_y}(\omega)\hat{y} + \tilde{G}_{p\star u_z}(\omega)\hat{z}$$

$$\vec{\tilde{G}}_{u\star p}(\omega) \equiv 2\vec{\tilde{S}}_{u\star p}(\omega) = 2\vec{\tilde{u}}^*(\omega)\cdot\tilde{p}(\omega) = \vec{\tilde{G}}^*_{p\star u}(\omega)$$
$$= \tilde{G}_{u_x\star p}(\omega)\hat{x} + \tilde{G}_{u_y\star p}(\omega)\hat{y} + \tilde{G}_{u_z\star p}(\omega)\hat{z}$$
$$= \tilde{G}^*_{p\star u_x}(\omega)\hat{x} + \tilde{G}^*_{p\star u_y}(\omega)\hat{y} + \tilde{G}^*_{p\star u_z}(\omega)\hat{z}$$

And for $\omega = 0$:

$$\tilde{G}_{p\star p}(0) \equiv \tilde{S}_{p\star p}(0) = \left|\tilde{p}(0)\right|^2 \text{ \{\textit{n.b.} a purely \underline{\textit{real}} quantity!\}}$$

$$\tilde{G}_{u\star u}(0) \equiv \tilde{S}_{u\star u}(0) = \left|\vec{\tilde{u}}(0)\right|^2 = 2\left[\left|\tilde{u}_x(0)\right|^2 + \left|\tilde{u}_y(0)\right|^2 + \left|\tilde{u}_z(0)\right|^2\right]$$
$$= \tilde{G}_{u_x\star u_x}(0) + \tilde{G}_{u_y\star u_y}(0) + \tilde{G}_{u_z\star u_z}(0) \text{ \{\textit{n.b.} in general, complex\}}$$

$$\vec{\tilde{G}}_{p\star u}(0) \equiv \vec{\tilde{S}}_{p\star u}(0) = \tilde{p}^*(0)\cdot\vec{\tilde{u}}(0) \text{ \{\textit{n.b.} in general, complex\}}$$
$$= \tilde{G}_{p\star u_x}(0)\hat{x} + \tilde{G}_{p\star u_y}(0)\hat{y} + \tilde{G}_{p\star u_z}(0)\hat{z}$$

$$\vec{\tilde{G}}_{u\star p}(0) \equiv \vec{\tilde{S}}_{u\star p}(0) = \vec{\tilde{u}}^*(0)\cdot\tilde{p}(0) = \vec{\tilde{G}}^*_{p\star u}(0) \text{ \{\textit{n.b.} in general, complex\}}$$
$$= \tilde{G}_{u_x\star p}(0)\hat{x} + \tilde{G}_{u_y\star p}(0)\hat{y} + \tilde{G}_{u_z\star p}(0)\hat{z}$$
$$= \tilde{G}^*_{p\star u_x}(0)\hat{x} + \tilde{G}^*_{p\star u_y}(0)\hat{y} + \tilde{G}^*_{p\star u_z}(0)\hat{z}$$

And for $\omega < 0$: All $\tilde{G}_{x\star y}(\omega) \equiv 0$ for $\omega < 0$, for $x, y = u, p$.

The ***frequency-domain*** complex 3-D vector acoustic intensity "amplitude" is:

$$\boxed{\vec{\tilde{I}}_a(\vec{r},\omega) \equiv \tfrac{1}{2}\tilde{p}(\vec{r},\omega)\cdot\vec{\tilde{u}}^*(\vec{r},\omega)}$$

Which, broken down into its 3 individual space components is:

$$\begin{aligned}\tilde{I}_{a_x}(\vec{r},\omega)\hat{x} &= \tfrac{1}{2}\tilde{p}(\vec{r},\omega)\cdot\tilde{u}_x^*(\vec{r},\omega)\hat{x}\\ \tilde{I}_{a_y}(\vec{r},\omega)\hat{y} &= \tfrac{1}{2}\tilde{p}(\vec{r},\omega)\cdot\tilde{u}_y^*(\vec{r},\omega)\hat{y}\\ \tilde{I}_{a_z}(\vec{r},\omega)\hat{z} &= \tfrac{1}{2}\tilde{p}(\vec{r},\omega)\cdot\tilde{u}_z^*(\vec{r},\omega)\hat{z}\end{aligned}$$

Hence, at the space-point $\vec{r}$:

$$\boxed{\vec{\tilde{I}}_a(\omega) = \tfrac{1}{2}\vec{\tilde{S}}_{u\star p}(\omega) = \tfrac{1}{2}\vec{\tilde{S}}^*_{p\star u}(\omega)} \Rightarrow \boxed{\vec{\tilde{I}}_a(\omega) = \vec{\tilde{G}}_{u\star p}(\omega) = \vec{\tilde{G}}^*_{p\star u}(\omega)} \text{ for } \omega > 0.$$

where:

$$\begin{aligned}\vec{\tilde{I}}_a(\omega) = \vec{\tilde{G}}_{u\star p}(\omega) &= \tilde{G}_{u_x\star p}(\omega)\hat{x} + \tilde{G}_{u_y\star p}(\omega)\hat{y} + \tilde{G}_{u_z\star p}(\omega)\hat{z}\\ = \vec{\tilde{G}}^*_{p\star u}(\omega) &= \tilde{G}^*_{p\star u_x}(\omega)\hat{x} + \tilde{G}^*_{p\star u_y}(\omega)\hat{y} + \tilde{G}^*_{p\star u_z}(\omega)\hat{z}\end{aligned}$$

Note that the complex 3-D vector specific acoustic ***impedance*** $\vec{\tilde{z}}_a(\vec{r},\omega)$ and ***admittance*** $\vec{\tilde{y}}_a(\vec{r},\omega) = 1/\vec{\tilde{z}}_a(\vec{r},\omega)$ are ***time-independent*** quantities. {They are in fact manifestly/intrinsically ***frequency domain*** quantities!}

Expressed in terms of their ***frequency domain*** definitions:

$$\begin{aligned}\vec{\tilde{z}}_a(\vec{r},\omega) \equiv \frac{\tilde{p}(\vec{r},\omega)}{\vec{\tilde{u}}(\vec{r},\omega)} &= \frac{\tilde{p}(\vec{r},\omega)}{\tilde{u}_x(\vec{r},\omega)}\hat{x} + \frac{\tilde{p}(\vec{r},\omega)}{\tilde{u}_y(\vec{r},\omega)}\hat{y} + \frac{\tilde{p}(\vec{r},\omega)}{\tilde{u}_z(\vec{r},\omega)}\hat{z}\\ &= \tilde{z}_{a_x}(\vec{r},\omega)\hat{x} + \tilde{z}_{a_x}(\vec{r},\omega)\hat{y} + \tilde{z}_{a_x}(\vec{r},\omega)\hat{z}\end{aligned}$$

and:

$$\begin{aligned}\vec{\tilde{y}}_a(\vec{r},\omega) \equiv \frac{\vec{\tilde{u}}(\vec{r},\omega)}{\tilde{p}(\vec{r},\omega)} &= \frac{\tilde{u}_x(\vec{r},\omega)}{\tilde{p}(\vec{r},\omega)}\hat{x} + \frac{\tilde{u}_y(\vec{r},\omega)}{\tilde{p}(\vec{r},\omega)}\hat{y} + \frac{\tilde{u}_z(\vec{r},\omega)}{\tilde{p}(\vec{r},\omega)}\hat{z}\\ &= \tilde{y}_{a_x}(\vec{r},\omega)\hat{x} + \tilde{y}_{a_y}(\vec{r},\omega)\hat{y} + \tilde{y}_{a_z}(\vec{r},\omega)\hat{z}\end{aligned}$$

Note also that:

$$\begin{aligned}\vec{\tilde{z}}_a(\vec{r},\omega) &= \frac{\tilde{p}(\vec{r},\omega)}{\tilde{u}_x(\vec{r},\omega)}\cdot\frac{\tilde{u}_x^*(\vec{r},\omega)}{\tilde{u}_x^*(\vec{r},\omega)}\hat{x} + \frac{\tilde{p}(\vec{r},\omega)}{\tilde{u}_y(\vec{r},\omega)}\cdot\frac{\tilde{u}_y^*(\vec{r},\omega)}{\tilde{u}_y^*(\vec{r},\omega)}\hat{y} + \frac{\tilde{p}(\vec{r},\omega)}{\tilde{u}_z(\vec{r},\omega)}\cdot\frac{\tilde{u}_z^*(\vec{r},\omega)}{\tilde{u}_z^*(\vec{r},\omega)}\hat{z}\\ &= \frac{2\tilde{I}_{a_x}(\vec{r},\omega)}{|\tilde{u}_x(\vec{r},\omega)|^2}\hat{x} + \frac{2\tilde{I}_{a_y}(\vec{r},\omega)}{|\tilde{u}_y(\vec{r},\omega)|^2}\hat{y} + \frac{2\tilde{I}_{a_z}(\vec{r},\omega)}{|\tilde{u}_z(\vec{r},\omega)|^2}\hat{z}\end{aligned}$$

The $k = x, y, z$ components of the ***frequency*** ***domain*** complex 3-D vector ***specific*** ***immittances*** at the listener's position $\vec{r}$ are:

$$\tilde{z}_{a_k}(\omega)=\frac{\tilde{p}(\omega)}{\tilde{u}_k(\omega)}=\frac{\tilde{u}_k^*(\omega)\cdot\tilde{p}(\omega)}{\tilde{u}_k^*(\omega)\cdot\tilde{u}_k(\omega)}=\frac{\tilde{u}_k^*(\omega)\cdot\tilde{p}(\omega)}{\left|\tilde{u}_k(\omega)\right|^2}=\frac{2\tilde{I}_{a_k}(\omega)}{\left|\tilde{u}_k(\omega)\right|^2}=\frac{\tilde{S}_{u_k\star p}(\omega)}{\tilde{S}_{u_k\star u_k}(\omega)}=\frac{\tilde{G}_{u_k\star p}(\omega)}{\tilde{G}_{u_k\star u_k}(\omega)}=\frac{\tilde{G}^*_{p\star u_k}(\omega)}{\tilde{G}_{u_k\star u_k}(\omega)}$$

and:

$$\tilde{y}_{a_k}(\omega)=\frac{1}{\tilde{z}_{a_k}(\omega)}=\frac{\tilde{u}_k(\omega)}{\tilde{p}(\omega)}=\frac{\tilde{u}_k(\omega)\cdot\tilde{p}^*(\omega)}{\tilde{p}(\omega)\cdot\tilde{p}^*(\omega)}=\frac{2\tilde{I}_{a_k}(\omega)}{\left|\tilde{p}(\omega)\right|^2}=\frac{\tilde{S}_{p\star u_k}(\omega)}{\tilde{S}_{p\star p}(\omega)}=\frac{\tilde{G}_{p\star u_k}(\omega)}{\tilde{G}_{p\star p}(\omega)}=\frac{\tilde{G}^*_{u_k\star p}(\omega)}{\tilde{G}_{p\star p}(\omega)}$$

Since $\tilde{y}_{a_k}(\vec{r},\omega)=1/\tilde{z}_{a_k}(\vec{r},\omega)$, we also see that:

$$\tilde{z}_{a_k}(\omega)=\frac{\tilde{G}_{u_k\star p}(\omega)}{\tilde{G}_{u_k\star u_k}(\omega)}=\frac{\tilde{G}^*_{p\star u_k}(\omega)}{\tilde{G}_{u_k\star u_k}(\omega)}=\frac{1}{\tilde{y}_{a_k}(\omega)}=\frac{\tilde{G}_{p\star p}(\omega)}{\tilde{G}_{p\star u_k}(\omega)}=\frac{\tilde{G}_{p\star p}(\omega)}{\tilde{G}^*_{u_k\star p}(\omega)}$$

Thus, we also see that:

$$\tilde{G}_{p\star p}(\omega)\cdot\tilde{G}_{u_k\star u_k}(\omega)=\tilde{G}_{p\star u_k}(\omega)\cdot\tilde{G}_{u_k\star p}(\omega)=\tilde{G}^*_{u_k\star p}(\omega)\cdot\tilde{G}^*_{p\star u_k}(\omega)=\left|\tilde{I}_{a_k}(\omega)\right|^2$$

We can also define corresponding $k = x, y, z$ vector components of the ***frequency***-***domain*** complex 3-D vector ***sound*** ***field*** ***coherence*** ***function*** $\vec{\tilde{\gamma}}_{p\star u_k}(\omega)$ {*n.b.* essentially the normalized (& dimensionless) complex 3-D vector acoustic intensity} as:

$$\vec{\tilde{\gamma}}_{u_k\star p}(\omega)\equiv\frac{\vec{\tilde{S}}_{u_k\star p}(\omega)}{\sqrt{\tilde{S}_{p\star p}(\omega)\cdot\tilde{S}_{u_k\star u_k}(\omega)}}=\frac{\vec{\tilde{G}}_{u_k\star p}(\omega)}{\sqrt{\tilde{G}_{p\star p}(\omega)\cdot\tilde{G}_{u_k\star u_k}(\omega)}}$$

where:

$$\vec{\tilde{\gamma}}_{u\star p}(\omega)=\tilde{\gamma}_{u_x\star p}(\omega)\hat{x}+\tilde{\gamma}_{u_y\star p}(\omega)\hat{y}+\tilde{\gamma}_{u_z\star p}(\omega)\hat{z}$$

Note that the ***magnitudes*** of the individual $k = x, y, z$ components of the ***frequency***-***domain*** complex 3-D vector ***sound*** ***field*** ***coherence*** ***function*** are constrained to lie within the range: $0\le\left|\tilde{\gamma}_{u_k\star p}(\omega)\right|\le 1$, *i.e.* the individual $k = x, y, z$ vector components are constrained to lie on, or within the ***unit*** ***circle*** in the complex plane, centered at (0,0).

When $\left|\tilde{\gamma}_{u_k\star p}(\omega)\right|\simeq 1$, the k^{th} component of a polyphonic complex sound field $\tilde{S}(\vec{r},t;\omega)$ is ***fully***-***coherent*** (*e.g.* at a listener's position *r* some distance away from a point sound source), whereas when $\left|\tilde{\gamma}_{u_k\star p}(\omega)\right|\simeq 0$, the k^{th} component of a polyphonic complex sound field is ***completely*** ***incoherent*** (*e.g.* at a listener's position deep inside the ***reverberant*** portion of a polyphonic complex sound field $\tilde{S}(\vec{r},t;\omega)$ associated with a large listening room and/or auditorium, concert hall, *etc*.).

Note further that when the {absolute value} of $\text{Re}\left\{\tilde{\gamma}_{u_k \star p}(\omega)\right\} \simeq 1$, the k^{th} component of a polyphonic complex sound field $\tilde{S}(\vec{r},t;\omega)$ is ***fully-coherent***, .and. is one that is associated with ***propagating*** sound radiation, *e.g*. when a listener's position is far from a point sound source, in the so-called ***far-field*** region of a sound source, $r \gg \lambda$.

However, when the {absolute value} of $\text{Im}\left\{\tilde{\gamma}_{u_k \star p}(\omega)\right\} \simeq 1$ the k^{th} component of a polyphonic complex sound field $\tilde{S}(\vec{r},t;\omega)$ is {also} ***fully-coherent***, but is instead associated with ***non-propagating*** sound radiation – *i*.e. acoustic energy that is simply sloshing back and forth locally at the listener's point *r* during each cycle of oscillation, *e.g*. in the so-called ***near-field*** region of a sound source, $r \ll \lambda$.

Thus, *e.g*. simultaneously exciting the 3 acoustic standing waves associated with the [1,0,0]/[0,1,0]/[0,0,1] axial modes of a cubical 3-D enclosure of side $d = \lambda/2$, with 3-fold degenerate modal frequency $f_{res} \equiv f_{100} = f_{010} = f_{001} = c/2d$, we see that $\text{Re}\left\{\tilde{\gamma}_{u_k \star p}(\omega_{res})\right\} \simeq 0$ and $\text{Im}\left\{\tilde{\gamma}_{u_k \star p}(\omega_{res})\right\} \simeq 1$ for each of the *k* = *x*, *y*, *z* components of this complex sound field.

We can additionally define the corresponding *k* = *x*, *y*, *z* vector components of the ***magnitude-squared*** version of the ***frequency-domain sound field coherence function*** $\left|\vec{\tilde{\gamma}}_{u\star p}(\omega)\right|^2$ {*n.b*. a purely ***real*** quantity}, as:

$$\left|\vec{\tilde{\gamma}}_{u\star p}(\omega)\right|^2 \equiv \vec{\tilde{\gamma}}_{u\star p}(\omega)\cdot\vec{\tilde{\gamma}}^{*}_{u\star p}(\omega) = \frac{\left|\vec{\tilde{S}}_{u\star p}(\omega)\right|^2}{\tilde{S}_{p\star p}(\omega)\cdot\tilde{S}_{u_k\star u_k}(\omega)} = \frac{\left|\vec{\tilde{G}}_{u\star p}(\omega)\right|^2}{\tilde{G}_{p\star p}(\omega)\cdot\tilde{G}_{u_k\star u_k}(\omega)}$$

where:

$$\left|\vec{\tilde{\gamma}}_{u\star p}(\omega)\right|^2 = \left|\tilde{\gamma}_{u_x\star p}(\omega)\right|^2 + \left|\tilde{\gamma}_{u_y\star p}(\omega)\right|^2 + \left|\tilde{\gamma}_{u_y\star p}(\omega)\right|^2$$

The individual *k* = *x*, *y*, *z* components of the ***frequency-domain*** the ***magnitude-squared*** coherence function $\left|\vec{\tilde{\gamma}}_{u\star p}(\omega)\right|^2$ can range from $0 \le \left|\tilde{\gamma}_{u_k\star p}(\omega)\right|^2 \le 1$. When $\left|\tilde{\gamma}_{u_k\star p}(\omega)\right|^2 \simeq 1$, a polyphonic complex sound field $\tilde{S}(\vec{r},t;\omega)$ is ***fully-coherent*** (*e.g*. at a listener's position some distance away from a single sound source), whereas when $\left|\tilde{\gamma}_{u_k\star p}(\omega)\right|^2 \simeq 0$, the polyphonic complex sound field is ***completely incoherent*** (*e.g*. at a listener's position deep inside the ***reverberant*** portion of a polyphonic complex sound field $\tilde{S}(\vec{r},t;\omega)$ associated with a large listening room and/or auditorium, concert hall, *etc*.).

It can also be seen from the above discussion(s) that the complex 3-D vector coherence function $\vec{\tilde{\gamma}}_{u_k\star p}(\omega)$ contains more information (real and imaginary components) and is thus more useful than its purely-real, magnitude-squared version $\left|\vec{\tilde{\gamma}}_{u\star p}(\omega)\right|^2$.

<u>Legal Disclaimer and Copyright Notice:</u>

<u>Legal Disclaimer:</u>

The author specifically disclaims legal responsibility for any loss of profit, or any consequential, incidental, and/or other damages resulting from the mis-use of information contained in this document. The author has made every effort possible to ensure that the information contained in this document is factually and technically accurate and correct.

<u>Copyright Notice:</u>

The contents of this document are protected under both United States of America and International Copyright Laws. No portion of this document may be reproduced in any manner for commercial use without prior *<u>written</u>* permission from the author of this document. The author grants permission for the use of information contained in this document for *<u>private</u>*, *<u>non-commercial</u>* purposes only.